# Sensitivity Analysis of Manufacturing Tolerances in Permanent Magnet Synchronous Machines With Stator Segmentation

J. Kolb and K. Hameyer, *Senior Member, IEEE*

***Abstract*—In this article the sensitivity of manufacturing tolerances on the output of a permanent magnet synchronous machine with stator segmentation is studied. To reduce the simulation effort, a transition of the stator segment air gaps to replacement geometry was applied and the relevant parameters are discussed, whereas the uncertainty of geometric and material parameters is modeled with a normal distribution. Furthermore, tolerance chains are expressed through the convolution of independent probability distributions. For the Design of Experiments Sobol sequences are utilized. To further decrease the number of design parameters an approach is presented to reduce redundant parameters to individual design parameters. For the sensitivity analysis the torque and torque ripple serve as quality objectives. In addition, an approach is revealed to use the variance of the radial forces as quality objective without considering mechanical FE simulations. For manufacturing tolerances a linear regression is satisfying to describe the main effects on the quality objectives. Repetitive machine parameters, e.g. the remanences, have less influence on the machine's output than particular parameters such as the housing radius or static eccentricity. The influences of stator segmentation are negligibly small, whereas the housing radius has the highest sensitivity on the machine's output.**

***Index Terms*—Design of experiments, finite element analysis, manufacturing tolerances, parameter reduction, sensitivity analysis, sobol sequences, stator segmentation, synchronous machine.**

## I. Introduction

ELECTRICAL machines, particularly permanent magnet synchronous machines (PMSM), have a large number of tolerance affected parameters. The resulting uncertainties from manufacturing processes could be apparent in certain circumstances in torque, torque ripple and in the noise exciting radial force waves, which can lead to vibrations in the stator housing.

This can increase ripple and noise to a point, where an electrical machine is considered as a faulty product and is sorted out at End-of-Line tests or as a return by customers, which can result in production waste or high costs for replacement. This time effort and costs can be reduced by considering manufacturing tolerances in the design phase of the machine.

However, it is not sufficient to tighten all tolerances, which can be time and cost consuming for the manufacturing process. Therefore only the tolerances have to be tightened, which will have the most influence on noise and ripple and in contrary tolerances with no significant influence can be widened. This will reduce tolerance induced deviations while lowering manufacturing costs.

In most studies limited parameters of the machine are investigated on only one machine output variable, e.g. the cogging torque, torque ripple or specific harmonics. Magnetization faults are studied, which can potentially result in significant cogging torque [1]. Another study investigates the influence of stator core assemblies on cogging torque [2]. Furthermore the effects of eccentricity on torque and radial force density are studied [3], [4]. Also the rotor misalignment faults on cogging torque are analyzed [5]. There are other studies, where manufacturing tolerances are investigated and individual parameters varied by their tolerance limits. For an advanced torque control, manufacturing tolerances are considered in Finite Element Analysis (FEA) to extract lumped parameters [6]. Further studies conceive the influence of rotor and stator deviations on torque and particular radial force harmonics [7], [8]. From series production measurements also torque deviations are deduced, which are caused by manufacturing tolerances [9]. Among others, magnet uncertainties are subject of research [10], [11].

In the research subject of global Sensitivity Analysis (SA), the term of the applied method in the presented studies are called One-factor-At-a-Time (OAT) analysis, where particular effects of uncertain parameters are studied, but combined influences are often neglected [12]. To comprise interactions between different parameters a global SA should be employed [13]. Only a few studies were published, that already performed the analysis with stochastic approaches [14], [15]. If analyzed, only particular radial force harmonics are investigated but not the entire harmonics spectrum, which can distort the belonging sensitivity measure.

None of the presented studies investigate interdependencies between manufacturing tolerances on torque, torque ripple and the harmonic spectrum and consider the probability distributions of the manufacturing tolerances, but which are important to obtain the proper sensitivities of manufacturing tolerances. Interdependencies of individual manufacturing tolerances with stator

Manuscript received January 15, 2020; revised May 5, 2020 and June 30, 2020; accepted August 3, 2020. Date of publication August 18, 2020; date of current version November 24, 2020. This work was supported by the German Research Foundation (DFG) within the research project number 323896285, "Propagation of uncertainties across electromagnetic models". Paper no. TEC-00059-2020. *(Corresponding author: Johann Kolb.)*

The authors are with the Institute of Electrical Machines (IEM), RWTH Aachen University, 52062 Aachen, Germany (e-mail: johann.kolb@iem.rwth-aachen.de; kay.hameyer@iem.rwth-aachen.de).

Color versions of one or more of the figures in this article are available online at https://ieeexplore.ieee.org.

Digital Object Identifier 10.1109/TEC.2020.3017279

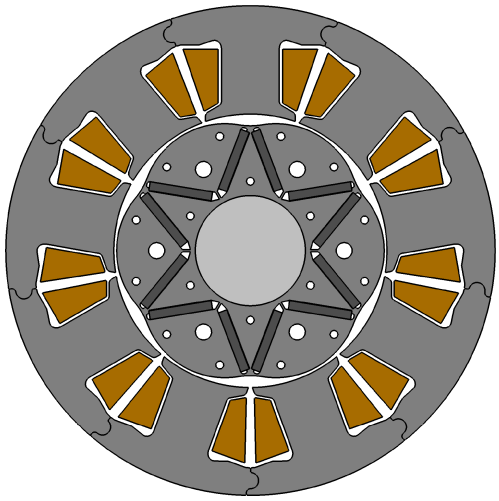

Fig. 1. Cross-section of the studied machine model.

segmentation are likewise not investigated. Hence, the objective of this study is to identify the most sensitive uncertain parameters regarding torque, torque ripples and radial force excitation. In contrast to the mentioned studies with OAT approaches, an extensive SA will be applied on the entire machine, combined with Design of Experiments (DOE) and magnetic FEA to comprise interactions of manufacturing tolerances. With this approach, this study contributes to develop a methodology to estimate the sensitivities for a large number of manufacturing tolerances and to evaluate the influence of the stator segmentation on the machine's output.

As machine a pump drive from series production will be investigated. Especially the noise of pumps through acoustic radiation or induced torque ripple in the pumping system can lead to undesired system behavior [17], [18]. The machine is introduced in Section II with uncertain manufacturing tolerances in Section III. The design of experiments with an algorithm for parameter reduction is presented in Section IV. The actual SA is depicted in Section V with a proposed method to comprise all force harmonics instead of investigating particular harmonics. The results are presented in Section VI and discussed in Section VII. Remarks are drawn in Section VIII.

## II. Machine Model

The studied machine is a permanent magnet synchronous machine with single tooth windings, stator segmentation and buried magnets (Fig. 1). The machine has a rated power of 4.5 kW and consists of three pole pairs with fractional slot windings (number of holes $q = 0.5$). Furthermore the rotor poles are formed as sinusoidal poles.

The machine is utilized as drive for pumps in large buildings for circulating domestic hot water. The pump system was already investigated as simulation model with lumped machine parameters and compared with measurements [16]. Because its application is stationary most of the time, FEA is driven at rated power with 4450 rpm and 9.6 Nm at a current amplitude of $\hat{I} = 10.0\text{A}$.

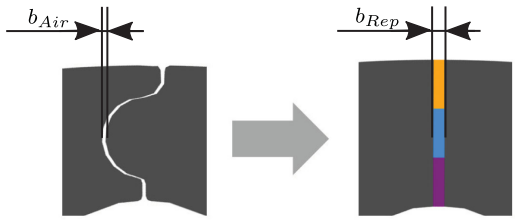


Fig. 2. Transition of the modeled stator segment air gap to replacement geometry.

### A. Replacement Geometry

Because influences of manufacturing tolerances on the forces in the rotor air gap are asymmetric, it is not sufficient to simulate a single pole pair, but the complete machine has to be comprised. Thus, the number of finite elements is very large and the simulation effort is not applicable for a sensitivity analysis.

To reduce the number of elements an adaptive mesh refinement is applied. It turned out, that the air gap transitions between the stator segments have to be meshed with a high resolution, where the elements measures few micrometers in size. To further reduce the number of elements, the segment air gaps could be defined by a replacement geometry so that the mesh generator produces significantly less elements and the solution does not change regarding the quality objectives.

The replacement geometry consists of three elements, so that a housing widening as well as a tilting of the stator segments can be simulated (Fig. 2). In magnetic equivalent circuit theory the magnetomotive force is calculated with a series of reluctance elements multiplied by magnetic flux. Here, it is used to calculate a new reluctance for the replacement geometry element. Because reluctance exhibits linear correlation with with the belonging element length, a linear scaling between electrical steel reluctance $R_{m,Steel}$ and segment air gap reluctance $R_{m,Air}$ is permissible [19].

Thus, the reluctivity of the replacement material can be described as

$$R_{m,Rep}(B) = R_{m,Steel}(B) \cdot \left(1 - \frac{b_{Air}}{b_{Rep}}\right) + R_{m,Air} \cdot \frac{b_{Air}}{b_{Rep}}. \quad (1)$$

$b_{Air}$ defines the segment air gap width and $b_{Rep}$ the width of the replacement gap between stator segments. $b_{Air}$ can be influenced by cutting tolerances, the housing radius $r_H$ as well as the tilting of the stator teeth.

The deviations between original and replacement geometry were computed for a machine without segment air gaps ($b_{Air} = 0.0$) and maximum segment air gap. The number of elements is reduced by $14.8\%$ between original and replacement geometry. The resulting accuracy for the quality objectives (see Section V-A) are depicted in Table I as ratio of quality objectives between FE mesh with replacement and original geometry, e.g the mean torque of the replacement geometry divided by the mean torque of the original geometry. The corresponding flux densities are

TABLE I
REPLACEMENT GEOMETRY ACCURACY AS RELATION BETWEEN QUALITY OBJECTIVES FOR REPLACEMENT AND ORIGINAL GEOMETRY

| Quality objective | Without air gap | Maximum segment air gap |
|---|---|---|
| $\overline{T}$ | 100.82% | 99.40% |
| $T_R$ | 101.00% | 98.59% |
| $\sigma^2_{rad}$ | 102.43% | 99.07% |

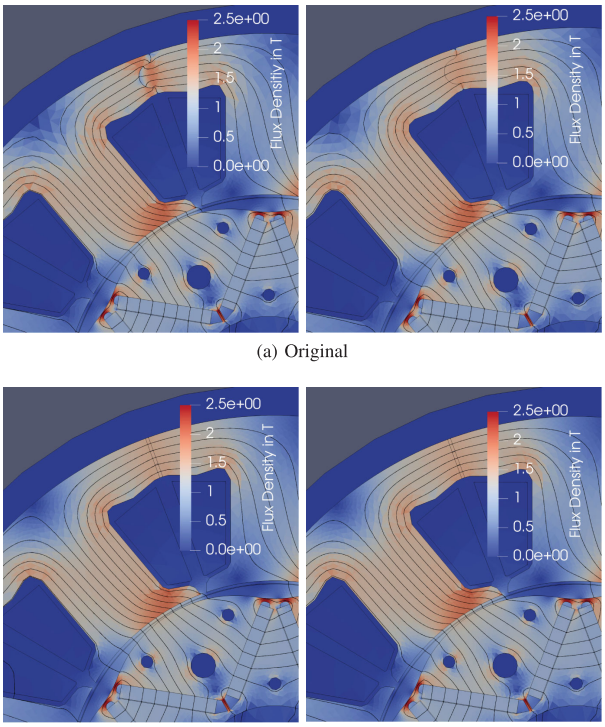


(a) Original

(b) Replacement

Fig. 3. Flux density with maximum segment air gap (left) and without air gap (right).

shown in Fig. 3. The local flux differs in the segment air gaps, but not significantly for the flux in the rotor air gap, which is relevant for force calculation. With maximum segment air gaps the quality objectives vary between $-0.6\%$ and $-1.4\%$ for original and replacement FEA. Without an segment air gap the variation is even higher with 0.82% to 2.34%, which could also be influenced by mesh discretization errors. Thus, the FEA with replacement geometry is feasible for the sensitivity analysis. The particular meshes are then created with a static mesh refinement.

### B. Force Calculation

The most important output of the machine are the tangential $F_{tan}$ and radial forces $F_{rad}$. Therefore, radial and tangential force densities are obtained from the flux density solution

$$\sigma_{Frad}(\alpha,t) = \frac{1}{2\mu_0} B^2_{rad}(\alpha,t) \tag{2}$$

$$\sigma_{Ftan}(\alpha,t) = \frac{1}{\mu_0} B_{rad}(\alpha,t) B_{tan}(\alpha,t) \tag{3}$$

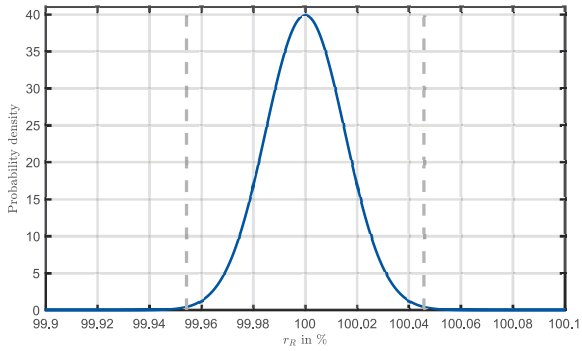


Fig. 4. Probability density of the rotor radius related to nominal radius. The dashed lines define the tolerance limits.

with radial $B_{rad}(\alpha,t)$ and tangential $B_{tan}(\alpha,t)$ flux density. $\alpha$ represents here the spatial angle, $t$ the temporal dependency and $\mu_0$ the vacuum permeability [4].

The torque $T(t)$ is deduced as integral of the tangential force density $\sigma_{Ftan}$, which is assumed to be invariant in axial direction and thus sufficient for radial field electrical machines and multiplied with the rotor radius $r_R$ and the active machine length $l$ [4].

$$T(t) = r_R^2\, l \int_0^{2\pi} \sigma_{Ftan}(\alpha,t)\, d\alpha \tag{4}$$

The radial force density can be depicted as force density waves, which yields by spatial and temporal Fourier decomposition to

$$\sigma_{Frad}(\nu,f) = \sum_s \sum_r \hat{\sigma}_{sr} \cos\left(\nu_s \alpha - 2\pi f_r t - \Phi_s\right), \tag{5}$$

where $\hat{\sigma}_{sr}$ represents the $s$-th spatial and temporal $r$-th force density wave amplitude, $f$ the frequency, $\nu$ the spatial order, $\nu_s$ the $s$-th spatial order, $f_r$ the $r$-th frequency order and $\Phi_s$ the phase shift angle [20], [21].

## III. UNCERTAIN MANUFACTURING PARAMETERS

In electrical machines a wide range of significant parameters exists, that influence the output and therefore the manufacturing quality of the machine. Geometric tolerances result from steel cutting processes and from assembling the lamination and material tolerances from a varying material composition [22], [23].

### A. Tolerance Distribution

In manufacturing processes geometric tolerances can mainly be considered as normal distributed [24]. Therefore the probability density of the distribution is described as

$$p(x) = \frac{1}{\sqrt{2\pi\sigma^2}} \exp\left(-\frac{(x-\mu)^2}{2\sigma^2}\right), \tag{6}$$

where $x$ is the length or radius of a component.

Fig. 4 shows the probability distribution of the rotor radius. As of empirical analysis the tolerance limits are set to $3\sigma$. Therefore $0.27\%$ of the manufactured rotors are out of the tolerance

TABLE II
UNCERTAIN MANUFACTURING PARAMETERS OF THE MACHINE

| Denotation | Parameter description | Quantity $k$ | Distribution type |
|---|---|---|---|
| $r_R$ | Rotor radius | 1 | normal |
| $l_M$ | Magnet length | 12 | normal |
| $w_M$ | Magnet width | 12 | normal |
| $B_R$ | Magnet remanence | 12 | normal |
| $w_{PM}$ | Magnet pocket width | 12 | normal |
| $b_M$ | Bridge between magnets | 12 | normal |
| $b_R$ | Bridge between magnets and outer rotor contour | 12 | normal |
| $h_T$ | Tooth height | 9 | normal |
| $\alpha_T$ | Tooth tilting | 9 | normal |
| $b_{Air}$ | Stator segment air gap | 9 | normal |
| $r_H$ | Housing inner radius | 1 | normal |
| $e_R$ | Displacement shaft to rotor contour | 1 | normal |
| $e_M$ | Displacement shaft mating surface | 1 | normal |
| $e_B$ | Bearing clearance | 1 | uniform |
| $e_S$ | Bearing seat displacement | 1 | normal |
| $e_H$ | Displacement stator to housing | 1 | normal |
| $\alpha_{Ecc,S}$ | Eccentricity angle | 1 | uniform |

specification. The manufacturing processes are comparable for all geometric tolerances, thus other tolerances are also set to $3\sigma$.

The relevant tolerances and their quantities in the machine are shown in Table II. Over all, there are 106 particular parameters which have to be considered. With the combination of tolerances, e.g. the eccentricity calculation, 103 manufacturing parameters are relevant for the sensitivity analysis. A repetitive tolerance will subsequently be mentioned as parameter class.

### B. Geometric Parameters

Geometric tolerances of the rotor are illustrated in Fig. 5a. The rotor radius $r_R$ is defined as outer radius of the sinusoidal rotor form. By increasing the radius the sinusoidal shape is extended uniformly. The geometrical dimensions of the magnets are defined by length $l_M$ and width $w_M$. On the inner side of the magnets are small surrounding air gaps for assembling purposes. The overall pocket width is consequently described as an independent parameter $w_{PM}$. Furthermore the flux barriers between the magnets $b_M$ and between the magnets and the outer contour of the rotor $b_R$ have to be comprised because of flux density concentration, which can influence the rotor air gap flux density.

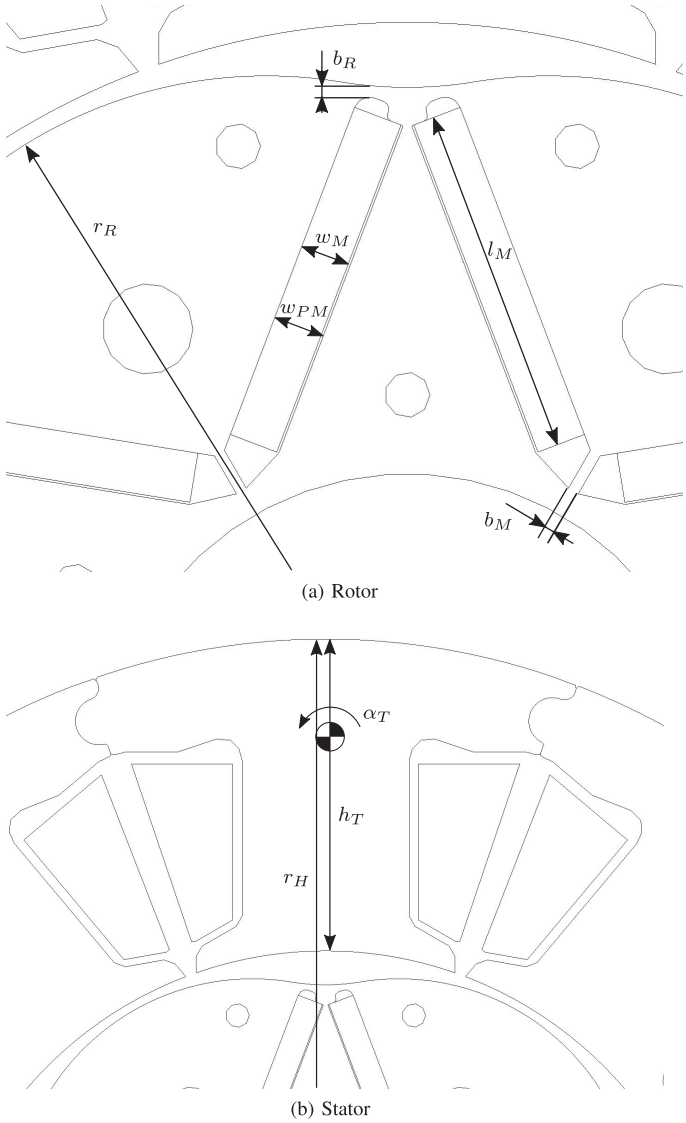


Fig. 5. Investigated geometric parameters.

The relevant parameters of the stator (Fig. 5b) include tooth height $h_T$ and tooth width $w_T$. The housing bore $r_H$ is also tolerance affected. When the stator is manufactured, the T-segments are pressed inside the housing and the segments fit tightly. If the bore is larger within the tolerance limits, the stator teeth move outward so that the rotor air gap increases. If a stator segment is manufactured smaller than other segments, but complies the tolerance limits, it could tilt, so that an edge of the tooth protrude into the rotor air gap. Hence, the segment tilting is also gathered as an independent parameter and is defined as angle $\alpha_T$.

The rotor eccentricity combines different individual tolerances. Therefore, the eccentricity is defined as closing dimension of a tolerance chain, which consists of the displacement between rotor shaft bore and outer contour $e_R$, the shaft mating surface for the rotor $e_M$, the bearing clearance $e_B$, the bearing seat in the end shield $e_S$ and the tolerance between housing and stator $e_H$. The

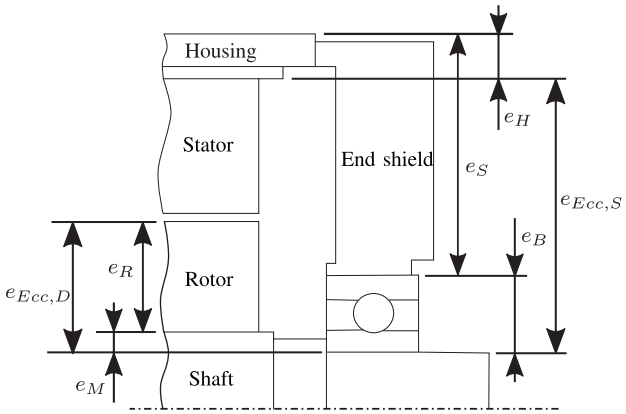


Fig. 6. Schematic longitudinal section of the machine.

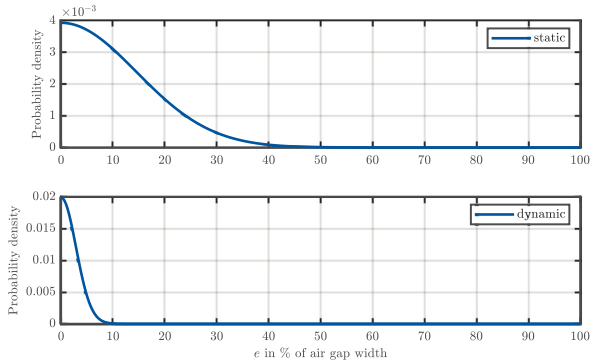


Fig. 7. Probability distributions of static and dynamic eccentricity.

longitudinal section in Fig. 6 illustrates the relations between the individual tolerances and eccentricities. The direction of the static eccentricity is defined as the eccentricity angle $\alpha_{Ecc,S}$.

The probability distribution $p_{Ecc,S}(x)$ of the static eccentricity $e_{Ecc,S}$ is here defined as convolution of probability distributions of the bearing clearance $p_B$, bearing seat in the end shield $p_S$ and the tolerance between housing and stator $p_H$:

$$p_{Ecc,S} = p_B * p_S * p_H. \tag{7}$$

This is permissible, because the particular parameters are considered as stochastically independent. The probability distribution $p_{Ecc,D}(x)$ of the dynamic eccentricity $e_{Ecc,D}$ is equally calculated as the convolution of probability distributions of the shaft mating surface for rotor $p_M$ and the outer diameter of the rotor $p_R$:

$$p_{Ecc,D} = p_M * p_R. \tag{8}$$

The resulting normal distributions are depicted in Fig. 7. The $3\sigma$ boundary of static eccentricity is reached at $43\%$ and the boundary of dynamic eccentricity at $9\%$ of the rotor air gap width.

The $3\sigma$ boundary of all geometric parameters are set their tolerance limits derived from technical drawings.

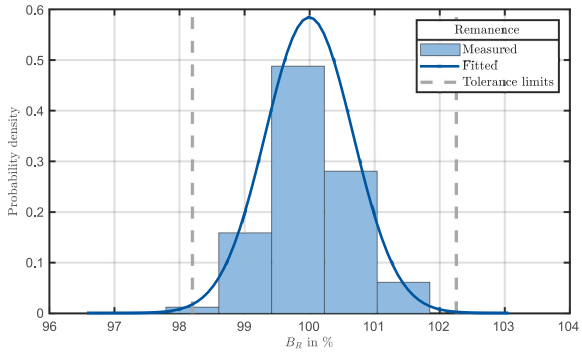


Fig. 8. Probability density of the magnet remanence.

### C. Material Parameters

Material uncertainties originate from deviations of the magnetization curve, losses of electrical steel and magnet remanence.

The magnetization curve and losses of electrical steel are influenced by a lot of different factors. Soft magnetic materials can vary in composition, but normal distributions are not sufficient for fitting. Electrical steel manufacturers only guarantee minimum properties for graded steel lamination materials, but do not define tolerance limits [25]. The magnetization properties are furthermore influenced by punching, welding and annealing [26], [27]. With different stacked and laminated stator segments, varying batches with deviations in material thickness and rolling directions also contribute to deterioration [28], [29]. Hence, the modeling of soft magnetic material including modeling of cutting edge effects, anisotropy and other deviations in magnetization and losses through manufacturing processes is an active research topic [30], [31]. Thus, the soft material modeling will be part of further investigations and is not scope of this study.

The remanence of the magnets $B_R$ is measured with 82 samples from series production so that a distribution can be fitted. The best fit is the normal distribution, which is estimated with the Maximum-Likelihood Estimation. In Fig. 8 the probability distribution over the remanence is shown. As a result, $0.42\%$ of the magnet remanence are larger or smaller than the manufacturers tolerances, determined with the limits in the specification sheet.

## IV. Design of Experiments

For generating the design samples for the Design Of Experiments (DOE) with probability distributed parameters, Sobol sequences are used [32]. Recent research revealed that for large multidimensional problems Quasi-Monte Carlo (QMC) methods, especially Sobol sequences, produce smaller probability errors than e.g. Halton sequences or classical methods like Latin Hypercube sampling [33], [34].

The Sobol sequence is based on the bit-wise calculation of the values for the design samples. To compute the $s$ dimension of the sampling point $j$ in the sequence, a $s_j$ degree primitive polynomial $Z$ is defined:

$$Z \equiv x^{s_j} + a_1 x^{s_j - 1} + \cdots + a_{s_j - 1} x + 1 \tag{9}$$

The coefficients $a_1, \ldots, a_{s_j-1}$ are chosen from $\{0, 1\}$. The polynomial in (9) is used to define the coefficient $m_k$:

$$m_k = 2a_1 m_{k-1} \oplus 2^2 a_2 m_{k-2} \oplus \ldots \oplus 2^{s_j-1} a_{s_j} m_{k-s_j+1} \oplus 2^{s_j} m_{k-s_j} \oplus m_{k-s_j}, \quad (10)$$

where $k > s_j$. The $\oplus$ operator denotes a bit-by-bit exclusive or operation. The initial values for $m_{k-s_j}, \ldots, m_k$ can be chosen freely with the constraint that $m_k$ is odd and $m_k < 2^{s_j}$.

The direction numbers $v_k$ are defined as

$$v_k = \frac{m_k}{2^k}. \quad (11)$$

Finally the sequence is computed with

$$x^n = b_1 v_1 \oplus b_2 v_2 \oplus \ldots, \quad (12)$$

where $\ldots b_3 b_2 b_1$ is the binary representation of $n$. Further details are specified in [32].

To comprise the probability distribution of certain design parameters, the resulting Sobol sequences are scaled with the inverse cumulative distribution function $P(x)^{-1}$ of the probability density $p(x)$ (see (6)):

$$x_p = P(x)^{-1}. \quad (13)$$

The detailed algorithm is described in [35].

### A. Algorithm for Parameter Reduction

To reduce the number of parameters, dependencies between different parameters of one parameter class are identified so that the parameter quantity is considerably reduced while maintaining the same significance for the analysis.

For example, if all magnet remanences as parameter class are directly included in the sensitivity analysis, the output would show the same influence to the quality objectives for all remanences because the magnets are arranged symmetrically and the probability distributions are equal for every magnet. Furthermore, the interferences between parameter classes are indeterminable and no certain combinations of parameter classes with particular large influence are visible, respectively.

Hence, the main idea is to find the minimum and maximum geometric influence on the quality objectives, so that the SA can be split in two with minimum and maximum geometric influence, respectively. Therefore, before computing the actual experimental design, the influence of all repetitive parameters are investigated for each parameter class. An obvious approach would be to employ a full factorial design to ascertain the geometric influence. If a $2^k$ full factorial design is generated for every parameter class, e.g. for the twelve remanences $k = 12$, there are $n = 4096$ possible combinations with a sequence of 0 and 1, representing minimum and maximum tolerance limits. But for the influence of each repetitive parameter, only combinations are relevant which are unique from each other because of the symmetric arrangement in the machine where only relative positions are relevant but not absolute positions.

For example, if there are four parameters with conditions 0 and 1, assuming that every parameter has the same influence and the arrangement is symmetric, the combination $b = [0011]_2$ (= $[3]_{10}$) exhibits the same influence to the quality objectives as $b = [0110]_2$ (= $[6]_{10}$), which is $[3]_{10}$ bit shifted to the left by 1 resulting in $[6]_{10}$. So the full factorial design can be reduced to patterns, which are unique and not symmetric to each other.

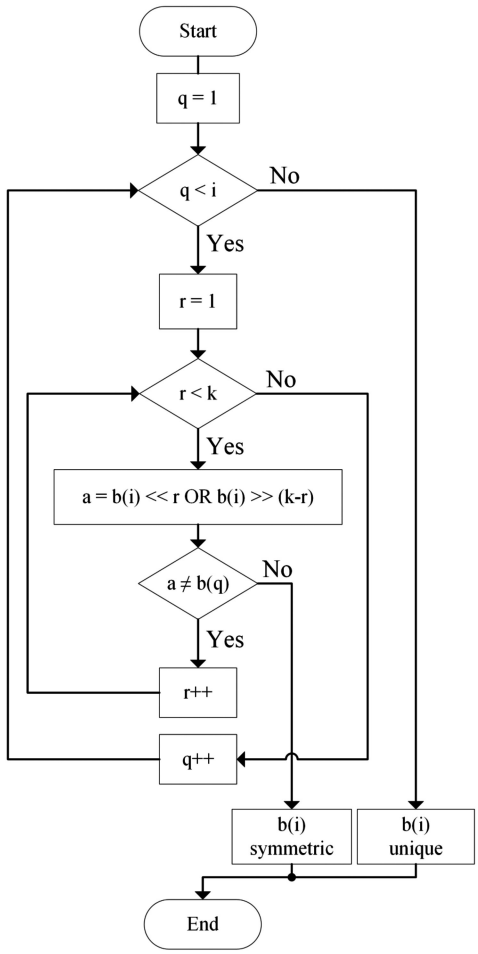


Fig. 9. Algorithm to study the uniqueness of a bit pattern after generating the bit pattern $b(i)$ with (14).

Thus, in the first stage the underlying rule can be formulated as

$$b(i) = \begin{cases} 0, & i = 1 \\ \sum_{j=2}^{i} 2^{j-2}, & i > 1 \end{cases}, i \in \mathbb{N} \cap i < 2^k, \quad (14)$$

where the bit sequence of $b(i) = [p_k \ldots p_3 p_2 p_1]$ represents the parameter pattern and $k$ is the amount of parameters.

In the second stage, the algorithm illustrated in Fig. 9 checks, if the bit representation of $b(i)$ is unique or symmetric to a another pattern of $b$. If the bit pattern is symmetric, then $b(i)$ is not a valid value of the numeric series.

The outer loop of the algorithm iterates over all unique bit patterns $b(q)$ that are smaller than $b(i)$ to check if $b(i)$ is symmetric to $b(q)$.

In the inner loop $b(i)$ is now compared to $b(q)$. Therefore $b(i)$ is bit shifted to the left by $r$ and to the right by $k - r$ and the results are then linked by a bitwise OR operation. If the variable equals $b(q)$, then $b(i)$ is symmetric to $b(q)$. If no symmetric

pattern is found, then $b(i)$ is marked as unique and it is considered as valid pattern for the pattern series.

Furthermore, all $b(i)$ are tested until $i$ is equal to $2^k$. At last, all unique $b(i)$ are now considered as reduced pattern series.

The pattern series count can be reduced to $n_b(k=9)=63$ and $n_b(k=12)=352$, which is $12.3\%$ and $8.6\%$ of the $2^k$ full factorial design, respectively. Applied to the parameter class of the remanence, the pattern series count is $n_b(k=12)=352$.

### B. Application of the Parameter Reduction

The algorithm for parameter reduction from Section IV-A is applied to each parameter from Table II with a quantity of more than one parameter as parameter class $c$, e.g. the remanence, while all other design parameters are set to their reference values. As a result, the minimum and maximum geometric influence of every parameter class is known, so that the sensitivity analysis can be split in two sets of DOE, where the influence of the geometric patterns are visible.

In a bit pattern 0 is set to the minimum tolerance limit and 1 to maximum tolerance limit of the belonging manufacturing parameter.

First, the FEA is applied for every $b(i)$ in the reduced pattern series. Then the quality objectives are calculated (see Section V-A). To find the overall geometric influence of parameter class $c$, the sum $\mathcal{Q}^{(c)}$ of all quality objects is calculated with quality objective $Q_m$, standardized by its standard deviation $\sigma$.

$$\mathcal{Q}^{(c)}(i)=\frac{\sum_{m=1}^{q}\sigma(Q_m^{(c)}(i))\cdot Q_m^{(c)}(i)}{\sum_{n=1}^{q}\sigma(Q_n^{(c)}(i))} \tag{15}$$

In the next step, the indexes of $max(\mathcal{Q}^{(c)}(i))$ and $min(\mathcal{Q}^{(c)}(i))$ are obtained as $i_{max}^{(c)}$ and $i_{min}^{(c)}$. The pattern with the minimum and maximum overall influence on the quality objectives are then selected as:

$$PP_{max}^{(c)}=b(i_{max}^{(c)}) \tag{16}$$

$$PP_{min}^{(c)}=b(i_{min}^{(c)}). \tag{17}$$

This approach is repeated for every parameter class $c$, so that a global minimum and maximum geometric pattern influence is achieved. In the last step, the geometric patterns are included into DOE for SA. Instead of considering a distribution for every individual parameter in a parameter class, one distribution $p_R$ for all parameters in the parameter class $c$ is utilized to reduce the design parameter count from $k$ to one. If the influence of one parameter $j$ in $PP^{(c)}$ equals 0, then the parameter is set to

$$x_{pn,j}^{(c)}=2x_N^{(c)}-x_p^{(c)}, \tag{18}$$

otherwise, if the parameter in $PP^{(c)}$ equals 1, the parameter is set to

$$x_{pp,j}^{(c)}=x_p^{(c)}. \tag{19}$$

$x_N^{(c)}$ describes here the nominal value of the belonging parameter class with $x_{pn}^{(c)}$ and $x_{pp}^{(c)}$ as adjusted distributed parameters and $x_p^{(c)}$ the DOE sample value of the belonging parameter class, obtained with the probability distribution $p_R^{(c)}$.

The original probability distribution $p(x)$ is only valid for one parameter, it therefore has to be adjusted to fit as a replacement for all parameters in a parameter class. Following the chain rule for independent probabilities, the probability distributions of all parameters in the parameter class have to be multiplied [37]. Because the distributions are equal, the resulting replacement distribution can be formulated as

$$p_R^{(c)}(x)=p(x)^{k^{(c)}}, \tag{20}$$

where $k^{(c)}$ is here the quantity of parameters in a parameter class $c$. Because of the exponentiation the resulting probability distribution is much steeper than for individual parameters.

There are now two different sets of DOE samples, one with minimum ($PP_{min}$) and one with maximum ($PP_{max}$) geometric pattern influence, which serve as inputs for SA with one parameter.

## V. Sensitivity Analysis

The sensitivity analysis comprises the consideration of significant quality objectives, a preinvestigation to further reduce the design parameters and a regression model as sensitivity measure. As described in Section IV-B minimum and maximum geometric pattern influences are here investigated as separate analyses to directly compare the influence of redundant geometric manufacturing parameters.

Different possibilities exist to obtain the sensitivity for input to output correlations. Like stated in the introduction global sensitivity analysis is an active research topic. The most popular sensitivity measure are the variance based Sobol Indices, which estimate first and second order sensitivities. The disadvantage of Sobol Indices are the fact, that a lot of design samples are required to obtain a meaningful analysis [12]. Furthermore, a method is presented to reduce the sample count, but for FEA it is even too high to apply [36].

If 500 samples are considered as sufficient to project the probability distributions of 9 design parameters on the quality objectives with a regression model, then 10000 samples for the same goodness are necessary with Sobol Indices. This sample count is not achievable with FEA. Therefore in further studies metamodels will be considered to estimate first and second order sensitivity indices. Hence, for this study, standard regression methods will be utilized.

### A. Quality Objectives

The output of the machine are radial and tangential tooth forces (see Section II). The sensitivity of the torque $T$ is measured as mean torque $\overline{T}$ and torque ripple $T_R$.

The mean torque for one rotation with the time period $\tau$ is calculated as

$$\overline{T}=\frac{1}{\tau}\int_0^{\tau}T(t)\,dt. \tag{21}$$

Furthermore, the torque ripple is defined as minimum to maximum peak torque related to the mean torque:

$$T_R=\frac{max(T(t))-min(T(t))}{2\overline{T}}. \tag{22}$$

TABLE III
INDIVIDUAL DESIGN PARAMETER INFLUENCES ON THE QUALITY OBJECTIVES RELATIVE TO NOMINAL VALUES (IN PERCENT)

| Denotation | $\overline{T}$ | | $T_R$ | | $\sigma^2_{rad}$ | |
|---|---|---|---|---|---|---|
| | min | max | min | max | min | max |
| $r_R$ | 99.57 | 100.43 | 98.86 | 101.14 | **102.75** | 97.35 |
| $l_M$ | 99.68 | 100.27 | 99.74 | 100.34 | 99.77 | 100.19 |
| $w_M$ | **97.84** | 101.78 | 98.17 | 102.12 | 98.46 | 101.21 |
| $w_{PM}$ | 99.43 | 100.69 | 99.14 | 100.75 | 99.56 | 100.49 |
| $b_M$ | 99.87 | 100.22 | 99.76 | 100.15 | 99.90 | 100.15 |
| $b_R$ | 99.71 | 100.37 | 99.02 | 100.77 | 99.75 | 100.29 |
| $h_T$ | 99.20 | 100.82 | 99.09 | **115.50** | 96.07 | 104.18 |
| $\alpha_T$ | 97.97 | 100.49 | 99.26 | **135.82** | 91.01 | 104.19 |
| $r_H$ | 96.89 | 100.00 | 95.49 | 100.00 | **85.41** | 100.00 |
| $e_{Ecc,S}$ | 100.00 | 101.37 | 92.41 | 100.00 | 100.00 | **121.07** |
| $e_{Ecc,D}$ | 100.00 | 100.03 | 99.66 | 100.00 | 100.00 | 100.08 |
| $B_R$ | 98.31 | 101.41 | 98.59 | **101.72** | 98.79 | 100.99 |
| $b_{Air}$ | 98.83 | 99.51 | **91.79** | 100.87 | 96.90 | 98.59 |

To appraise the acoustic radiation of the machine, the surface acceleration is usually calculated with structural dynamics simulations. To overcome the necessity of complete mechanical FEA for every sample, the influence of manufacturing parameters on the radial forces is estimated with the variance $\sigma^2_{rad}$ of spatial $s$ and temporal $r$ modes based on the sensitivity estimation with Fourier amplitude test sensitivity (FAST):

$$\sigma^2_{rad} = \frac{1}{2}\sum_{s=1}^{\infty}\sum_{r=1}^{\infty}(A^2_{sr} + B^2_{sr}), \tag{23}$$

where $A_{sr}$ and $B_{sr}$ are the complex Fourier coefficients of the force wave density (5) [37], [38]. Thus, only harmonics are included in the sensitivity measure and not the constant radial force component ($s = r = 0$).

### B. Preinvestigation

To further reduce the number of parameters, all design parameters with an overall influence on the quality objectives less than $1.0\%$ relative to nominal values are neglected. In Table III the influences of individual parameters are listed. For this, the machine is simulated with the minimum and maximum tolerance limits of every parameter, where the tolerance of all other parameters are set to their reference state. Parameters in parameter classes are set to their tolerance limits simultaneously.

The reference state for every quality objective is defined as $100\%$ so that tolerance limits are comparable. The highlighted values expose the highest absolute deviation. The magnet length $l_M$, magnet pocket width $w_{PM}$, bridges $b_M$ and $b_R$, and the dynamic eccentricity $e_{Ecc,D}$ show no significant influence on the quality objectives. Thus, these parameters are set to their reference state for the SA.

In Table IV the resulting design parameters for the sensitivity analysis are presented. The eccentricity angle $\alpha_{Ecc,S}$ is also specified as design parameter to evaluate the goodness of the experimental design. Because the parameter is uniformly distributed and varied between 0 and $2\pi$ within the design of experiments, single quality objectives differs, but with a $2\pi$ angle rotation, there should be no dependency of the angle in the stochastical analysis. With the parameters, which have a particular influence with more than $1\%$ on the quality objectives and the eccentricity angle, SA is performed with 9 parameters.

TABLE IV
INVESTIGATED MANUFACTURING PARAMETERS FOR THE SENSITIVITY ANALYSIS

| Denotation | Parameter description | Distribution type |
|---|---|---|
| $r_R$ | Rotor radius | normal |
| $w_M$ | Magnet width | normal |
| $h_T$ | Tooth height | normal |
| $\alpha_T$ | Tooth tilting | normal |
| $r_H$ | Housing inner radius | normal |
| $e_{Ecc,S}$ | Static eccentricity | normal |
| $\alpha_{Ecc,S}$ | Eccentricity angle | uniform |
| $B_R$ | Remanence | normal |
| $b_{Air}$ | Stator segment air gap | normal |

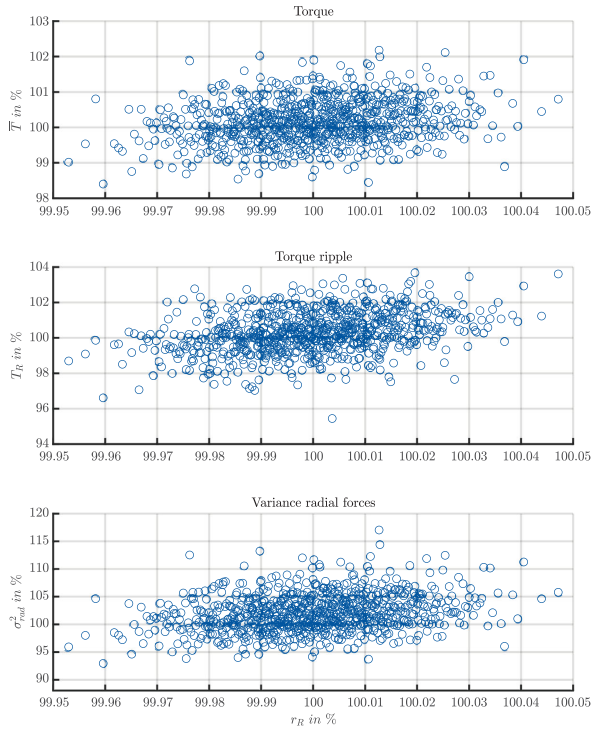


Fig. 10. Scatter plots of the rotor radius.

Fig. 10 shows the scatter plots of the rotor radius and Fig. 11 of the housing radius on the quality objectives. Because of the small deviations from the manufacturing tolerances, the mean rising of the quality objectives can be considered as linear. The depicted scatter plots confirm this hypothesis. The other design parameters likewise reveal this behavior. Another study on dimensional and material tolerances reveals the same linear correlation [39].

### C. Regression Model

As depicted in Section V-B, a linear regression model is sufficient to process the main dependencies.

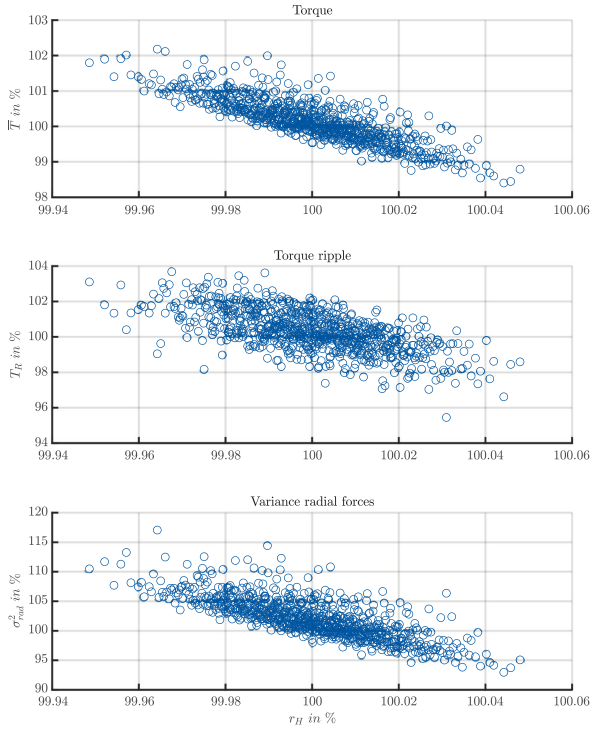


Fig. 11. Scatter plots of the housing radius.

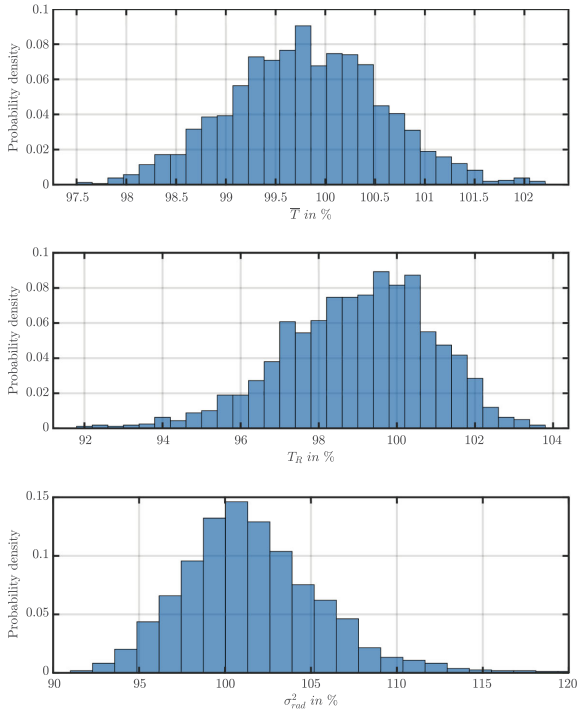


Fig. 12. Overall probability density of the quality objectives.

The linear model is defined as

$$\hat{y}_i(x_i) = \hat{\theta}_1 + \hat{\theta}_2\, x_i \tag{24}$$

with the regression coefficients $\hat{\theta}_1$ and $\hat{\theta}_2$.

The regression coefficients are calculated as the minimum of the sum of the squared distances between $(x_i, y_i)$ and $(x_i, \hat{y_i})$ [40].

$$\hat{\theta}_2 = \frac{\sum_{i=1}^{n}(x_i - \bar{x})(y_i - \bar{y})}{\sum_{i=1}^{n}(x_i - \bar{x})^2} \tag{25}$$

$$\hat{\theta_1} = \bar{y} - \hat{\theta}_2\, \bar{x} \tag{26}$$

For the sensitivity analysis the regression coefficient $\hat{\theta}_2$ is utilized. Because the different design parameters have different dimensions, the regression coefficient is standardized with

$$S = \hat{\theta}_2 \frac{\sigma_x}{\sigma_y}, \tag{27}$$

where $S$ is the sensitivity measure and $\sigma_x$ and $\sigma_y$ the standard deviations, which are the calculated with $x$ and $y$, respectively.

In the sensitivity analysis, $x$ represents one of the design parameters of Table IV and $y$ one of the quality objectives pointed out in Section V-A.

## VI. Results

The resulting regression coefficients for each design parameter in Table IV are depicted in Fig. 13. Fig. 13a shows the sensitivity analysis for the maximum geometric pattern $PP_{max}$ influence and Fig. 13b the analysis for the minimum geometric pattern influence $PP_{min}$ as discussed in Section IV-B. For each analysis 500 design samples are employed, which is satisfying to represent the design parameter distributions.

The inner housing radius $r_H$ shows a high negative correlation concerning torque, torque ripple, radial force variance. This results from an enlargement of the rotor air gap width because the stator segments have more space inside the housing and therefore are displaced outwards compared to the reference design. The rotor radius $r_R$ exhibits a positive correlation to the quality objectives, which is obviously yielding by decreasing the air gap width and increasing the air gap flux density.

The static eccentricity $e_{Ecc,S}$ influences the torque in a slightly positive direction because of the smaller one-sided air gap width while the torque ripple is decreasing. The radial forces variance shows a strong rise with increasing eccentricity. The eccentricity angle $\alpha_{Ecc,S}$ reveals the described behavior that the angle should converge to zero; the regression coefficient is nearly zero.

The magnet width $w_M$ shows a minor increase in torque for maximum geometric pattern influence and a minor decrease for minimum geometric pattern influence. The parameter has no significant influence on torque ripple and radial forces variance.

The remanence parameter $B_R$ has a minor influence on torque, but not significantly on the other quality objectives. With maximum geometric pattern influence the torque increases and with the minimum geometric pattern the parameter slightly decreases. For the maximum geometric pattern influence the height of the stator segment $h_T$ shows a small fall in torque ripple. The other quality objectives provide no significant correlation. The angle of the stator segments $\alpha_T$ yields to a minor contrary relation between torque, radial force variance and torque ripple which is more distinct with minimum geometric pattern influence.

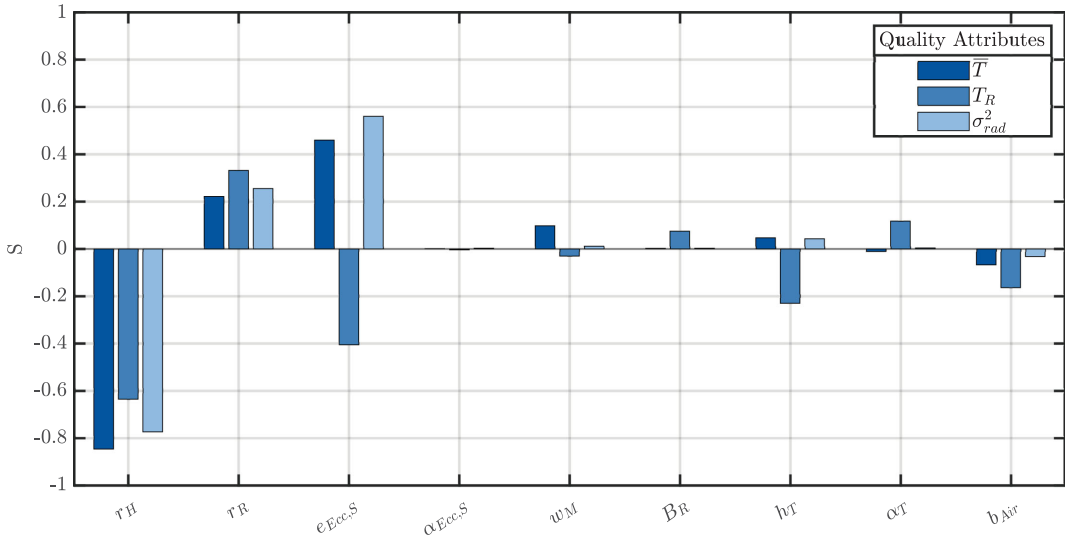


(a) Maximum geometric pattern influence $PP_{max}$

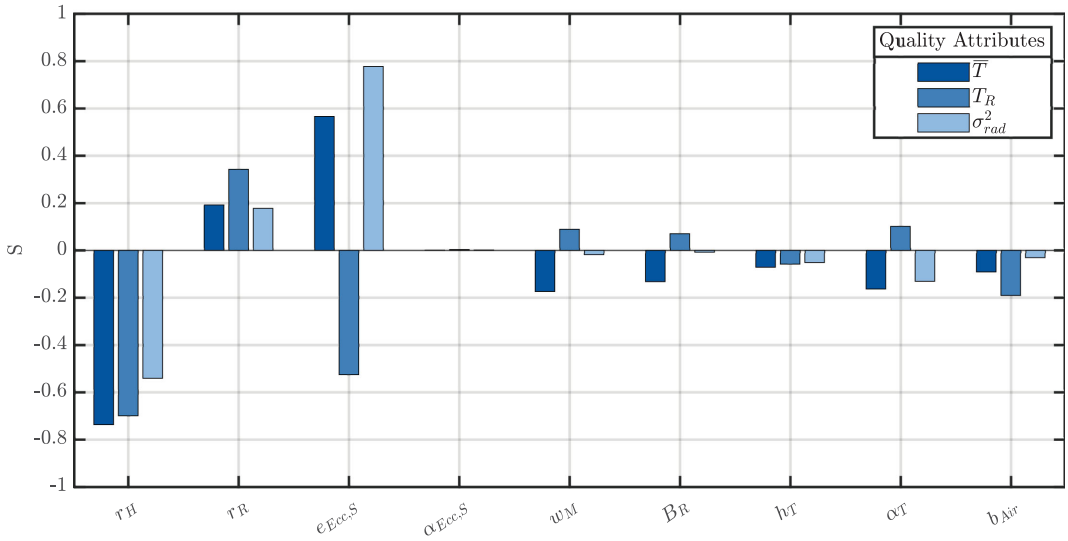


(b) Minium geometric pattern influence $PP_{min}$

Fig. 13. Sensitivity analysis for manufacturing parameters of Table IV.

The width of air gaps between stator segments $b_{Air}$ reduces all quality objectives in a minor way, but have no significant influence in contrast to eccentricity and housing radius.

The resulting overall probability density with all samples are shown in Fig. 12. Torque and torque ripple only have small variations within deviations of approximately $2.5\%$ and $5\%$ of the reference design. In contrast, the variance of radial forces reveals deviations up to $10\%$ of the reference design, but in some constellations the radial force variance can increase up to $15\%$ of the nominal value.

## VII. Discussions

The accuracy of the design of experiments is an important factor for the sensitivity analysis. With different estimation approaches such as the star discrepancy the design can be studied before the simulations are performed [33]. However, to be sure that the sensitivity analysis is reliable, the angle of eccentricity $\alpha_{Ecc,S}$ is included in the analysis. Because the parameter is uniformly distributed and should have no influence on the quality objectives, it is a good measure for the quality of the DOE. Like stated in the results (Section VI) the regression coefficient is nearly zero and therefore the results of SA are trustful. If the angle would have an influence on the results, then the sample count should be increased or algorithms and simulations should be checked for errors.

The analysis reveals a high impact of the eccentricity on the radial force variance. The resulting distribution is described in Section III-B and preinvestigated in Section V-B. The eccentricity can reach up to $43\%$ of the air gap width, where each

component of the tolerance chain is important for the resulting deviations. The overall probability density in Fig. 12 also reveals a high rise of the radial forces variance for some design samples, where the main influence is the static eccentricity. Thus, especially particular parameters with large tolerance limits, which are not inherent to a parameter class and therefore direct inputs for SA, need to be tightened to reduce the influence on the quality objectives.

Parameters, which are repetitive in the machine, e.g. the remanences of the magnets, have significant less influence than individual parameters as the eccentricity, rotor or housing radius (see Section IV-B). The height and tilting of the stator segments revealed high deviations for the torque ripple within the tolerance limits in the preinvestigation, but less influence in the sensitivity analysis. The stator segment air gaps have neither significant influences on the torque ripple, nor radial force variance. Hence, tolerance limits of individual manufacturing parameters have to be tightened and tolerance limits for repetitive parameters can be extended within its feasibility without risking significant loss in manufacturing quality concerning the quality objectives. In certain conditions the tilting angle air gap could have an influence and cannot be neglected beforehand. If the sensitives of eccentricity, housing and rotor radius are significantly higher than the sensitivities of tilting angle and segment air gap, in further studies the stator segments can be simulated in FEA as coherent object with a continuous yoke to reduce finite element size, simulation effort and the number of design parameters. Depending on the aim of further studies, the stator segment height has to be considered, which is also applicable with a continuous yoke.

The radial force variance as quality objective seems to be a good measure to evaluate the harmonics of radial forces. However, if the radial force variance indicate a strong rise for a design parameter, mechanical FEA has to be performed to compute the surface acceleration, which will reveal the actual influence of the acoustic radiation on the parameter. But in reverse, if the radial force variance shows no significant correlation to the design parameter, surface acceleration wont increase either, because structural dynamics are not excited by radial forces. Therefore the variance is a measure to evaluate the influence of force excitation harmonics, but not for acoustic radiation. In advance, design parameters without significant influence can be neglected in further investigations with an even higher simulation effort, e.g. when mechanical FE simulations are included.

## VIII. Conclusion

In this paper the influences of various manufacturing tolerances on the torque, torque ripple and radial forces are studied.

A permanent magnet synchronous machine with single tooth windings and segmented stator was described, including a method to reduce the number of finite elements by applying a replacement geometry for the air gap between the stator segments. The radial and tangential flux densities provide the basis to calculate the torque and radial forces, which will serve as inputs of the quality objectives for sensitivity analysis.

Subsequently, the uncertain manufacturing parameters were studied. Most manufacturing tolerances, which includes geometric and material tolerances, are normal distributed. To reduce the number of repetitive parameters in a machine, an approach is presented to calculate the sensitivity analysis with maximum and minimum geometric pattern influence.

To further reduce the design parameters, a preinvestigation is performed, where individual minimum and maximum influences are examined. Parameters with an influence less than one percent are set to their nominal value. In addition, an algorithm is presented to estimate the variance of the radial forces to conceive the radial force harmonics as one quality objective. Thus, torque, torque ripple and radial force variance are set as quality objectives. For sensitivity analysis a linear regression is utilized, which is sufficient for the analysis of manufacturing tolerances.

The analysis reveals high sensitivities for the housing and rotor radius as well as static eccentricity. Other parameters have significantly less influence on the quality objectives. Stator segment height, tilting angle and segment air gaps have minor influence, but cannot neglected beforehand, because in certain conditions the influence can rise. This can be determined with a preinvestigation.

If a manufacturing parameter is considered as repetitive in the machine, e.g. the remanence, the impact on the quality objectives is relatively small compared to individual parameters with large tolerances, which can have a high influence on torque and radial force harmonics.

## References


[1] I. Coenen, M van der Giet, K. Hameyer, "Manufacturing tolerances: Estimation and prediction of cogging torque influenced by magnetization faults," in *Proc. 14th Eur. Conf. Power Electron. Appl., EPE 2011*, pp. 1-9, Birmingham, UK, 2011.

[2] Z. Zhu, A. Thomas, J. Chen and G. Jewell, "Cogging torque in flux-switching permanent magnet machines," *IEEE Trans. Magn.*, vol. 45, no. 10, pp. 4708–4711, Oct. 2009.

[3] C. Schlensok and K. Hameyer, "Body-sound analysis of a power-steering drive considering manufacturing faults," *IEEE Trans. Veh. Technol., Vol. 56*, vol. 4, pp. 1553–1560, Jul. 2007.

[4] M. Schröder, D. Franck and K. Hameyer, "Analytical modeling of manufacturing tolerances for surface mounted permanent magnet synchronous machines," in *Proc. IEEE Int. Electric Mach. Drives Conf.*, pp. 1138–1144, Coeur d'Alène, Idaho, USA, May 2015.

[5] M. Thiele and G. Heins, "Computationally efficient method for identifying manufacturing induced rotor and stator misalignment in permanent magnet brushless machines," *IEEE Trans. Ind. Appl.*, vol. 52, no. 4, pp. 3033–3040, Jul.-Aug. 2016.

[6] M. Ott and J. Böcker, "Sensitivity analysis on production tolerances for electric drive systems in automotive application," *2016 18th Eu. Conf. Power Electron. Appl.*, pp. 1–10, Karlsruhe, Germany, 2016.

[7] C. Mülder, M. Franck, M. Schröder, M. Balluff, A. Wanke and K. Hameyer, "Impact study of isolated and correlated manufacturing tolerances of a permanent magnet synchronous machine for traction drives," in *Proc. IEEE Int. Electric Mach. Drives Conf.*, San Diego, CA, USA, 2019, pp. 982–987.

[8] M. Balluff, H. Naumoski and K. Hameyer, "Sensitivity analysis on tolerance induced torque fluctuation of a synchronous machine," in *Proc. 6th Int. Electric Drives Prod. Conf.*, Nov. 2016, pp. 128–134.

[9] G. Pfingsten, M. Hombitzer and K. Hameyer, "Influence of production uncertainties and operational conditions on torque characteristic of an induction machine," in *Proc. 5th Int. Electric Drives Prod. Conf*, - Nov. 2015, pp. 1–5.

[10] P. Offermann, I. Coenen, D. Franck and K. Hameyer, "Magnet deviation measurements and their consideration in electromagnetic field simulation," in *Proc. 15th IGTE Sympsium 2012*, Sep. 2012, pp. 305–309.

[11] L. Gasparin, A. Cernigoj, S. Markic and R. Fiser, "Additional cogging torque components in permanent-magnet motors due to manufacturing imperfections," *IEEE Trans. Magn.*, vol. 45, no. 3, pp. 1210–1213, Mar. 2009.

[12] A. Saltelli *et al.*, *Global Sensitivity Anal.: The Primer*, Sussex, England: John Wiley & Sons Ltd, 2008.
[13] F. Ferretti, A. Saltelli and S. Tarantola, "Trends in sensitivity analysis practice in the last decade," *Sci. The Total Environ.*, vol. 568, pp. 666–670, 2016.
[14] Y. Kim, J. Hong and J. Hur, "Torque characteristic analysis considering the manufacturing tolerance for electric machine by stochastic response surface method," *IEEE Trans. Ind. Appl.*, vol. 39, no. 3, pp. 713–719, May/Jun. 2003.
[15] P. Offermann, H. Mac, T. Nguyen, S. Clénet, H. De Gersem and K. Hameyer, 'Uncertainty quantification and sensitivity analysis in electrical machines with stochastically varying machine parameters," *IEEE Trans. Magn.*, vol. 51, no. 3, pp. 1–4, Mar. 2015.
[16] S. Schmuelling, O. Drubel, R. Ummelmann and M. de Zeeuw, "Combined method for simulation of high efficient circulating pumps," in *Proc. 2016 XXII Int. Conf. Elect. Mach.* , Lausanne, France, 2016, pp. 212–217.
[17] Y. Perriard, C. Koechli and L. Cardoletti, "Noise reduction for brushless DC motor-sensorless control analysis and back-EMF shape modification," in *Proc. IEEE 2002 28th Annual Conf. Ind. Electron. Soc. IECON 02*, Sevilla, Spain, 2002, pp. 1038–1043.
[18] T. Koenig and T. Wilharm, "Reducing magnetic noise of an auxiliary water pump drive," Innovative Small Drives and Micro-Motor Systems; 9. GMM/ETG Symposium, pp. 1–6, Germany, Nov. 2013.
[19] H. Polinder, J. Slootweg, M. Hoeijmakers and J. Compter, "Modelling of a linear PM machine including magnetic saturation and end effects: Maximum force to current ratio," in *Proc. IEEE Int. Elect. Mach Drives Conf., 2003*, Madison, WI, USA, 2003. pp. 805–811.
[20] M. van der Giet, R. Rothe, M. H. Gracia and K. Hameyer, "Analysis of noise exciting magnetic force waves by means of numerical simulation and a space vector definition," in *Proc. 18th Int. Conf. Electr. Mach.*, pp. 1-6, Vilamoura, Portugal, 2008.
[21] H. Jordan, *Geräuscharme Elektromotoren, Lärmbildung und Lärmbeseitung bei Elektromotoren*, Essen, Germany: W. Girardet, 1950.
[22] A. Kraemer, M. Veigel, P. Pontner, M. Doppelbauer and G. Lanza, "Influences of separation and joining processes on single tooth laminated stacks," in *Proc. 6th Int. Electric Drives Prod. Conf.*, Nov. 2016, pp. 178–185.
[23] M. Tietz, P. Biele, A. Jansen, F. Herget, K. Telger and K. Hameyer, "Application-specific development of non-oriented electrical steel for EV traction drives," in *Proc. 2nd Int. Electric Drives Prod. Conf.*, Nov. 2012, pp. 1–5.
[24] H. Brüggemann and P. Bremer, *Handbuch Qualitätsmanagement*, Wiesbaden, Berlin, Germany: Springer Fachmedien Wiesbaden, 2015.
[25] S. Sprague, "An examination of magnetic property variation of specification-acceptable electrical steel," in *Proc. 20th Int. Conf. Electr. Mach.*, Marseille, France, 2012, pp. 1172–1177.
[26] H. Weiss, P. Trober, R. Golle, S. Steentjes, S. Elfgen, K. Hameyer and W. Volk, "Impact of punching parameter variations on magnetic properties of non-grain oriented electrical steel," *IEEE Trans. On Ind. Appl.*, vol. 54, no. 6, pp. 5869–5878, Nov.–Dec. 2018.
[27] A. Krings, S. Nategh, O. Wallmark and J. Soulard, "Influence of the welding process on the performance of slotless PM motors with SiFe and NiFe stator laminations," *IEEE Trans. Ind. Appl.*, vol. 50, no. 1, pp. 296–306, Jan.–Feb. 2014.
[28] R. M. Strnat, M. J. Hall and M. S. Masteller, "Precision and accuracy study on measurement of soft magnetic properties using DC hysteresigraphs," *IEEE Trans. Magn.*, vol. 43, no. 5, pp. 1884–1887, May 2007.
[29] W. M. Arshad *et al.*, "Incorporating lamination processing and component manufacturing in electrical machine design tools," in *Proc. IEEE Ind. Appl. Annu. Meet.*, pp. 94–102, New Orleans, LA, 2007.
[30] S. Elfgen, S. Steentjes, S. Böhmer, D. Franck and K. Hameyer, "Continuous local material model for cut edge effects in soft magnetic materials," *IEEE Trans. Magn.*, vol. 52, no. 5, pp. 1–4, May 2016.
[31] F. Müller, G. Bavendiek, N. Leaning, B. Schauerte and K. Hameyer, "Consideration of ferromagnetic anisotropy in electrical machines built of segmented silicon steel sheets," in *Proc. Tenth Int. Conf. Comput. Electromagnetics*, pp. 1-6, Edinburgh, UK, 2019.
[32] P. Bratley and B. Fox, "Algorithm 659: implementing sobol's quasirandom sequence generator," in *ACM Trans. Math. Softw.*, vol. 14, 1988.
[33] X. Wang and I. Sloan, "Low discrepancy sequences in high dimensions: How well are their projections distributed?" *J. Comput. Appl. Mathematics*, vol. 213, no. 2, pp. 366–386, 2008.
[34] H. Niederreiter, *Random Number Generation and Quasi-Monte Carlo Methods*, vol. 63, USA: Society for Industrial and Applied Mathematics, 1992.
[35] J. Beasley and S. Springer: "Algorithm AS 111: The percentage points of the normal distribution," in *J. Roy. Stat. Soc.*, Series C, 1977.
[36] A. Saltelli *et al.*, "Variance based sensitivity analysis of model output. Design and estimator for the total sensitivity index," *Comput. Phys. Commun.*, vol. 181, no. 2, pp 259–270, 2010.
[37] R. Cukier, H. Levine and K. Shuler, "Nonlinear sensitivity analysis of multiparameter model systems," *J. Comput. Phys.*, vol. 26, no. 1, pp. 1–42, 1978.
[38] A. Saltelli and R. Bolado, "An alternative way to compute Fourier amplitude sensitivity test (FAST)," *Comput. Statist. Data Anal.*, vol. 26, no. 4, pp. 445–460, 1998.
[39] N. Taran, V. Rallabandi, D. M. Ionel, P. Zhou, M. Thiele and G. Heins, "A systematic study on the effects of dimensional and materials tolerances on permanent magnet synchronous machines based on the IEEE Std 1812," *IEEE Trans. Ind. Appl.*, vol. 55, no. 2, pp. 1360–1371, March/April 2019.
[40] C. Czado and T. Schmidt, *Mathematische Statistik*, Heidelberg, Germany: Springer-Verlag Berlin Heidelberg, 2011.

**Johann Kolb** received the M.Sc. degree in mechanical engineering from the University of Rostock, Germany in May 2017. He has been working as a Research Associate at the Institute of Electrical Machines (IEM), RWTH Aachen University since November 2017. His research interests include the simulation and analysis of electrical machines as well as the condition monitoring of electrical powertrains.

**Kay Hameyer** (Senior Member, IEEE) received the M.Sc. degree in electrical engineering from the University of Hannover, Germany, in 1986, his Ph.D. degree from University of Technology Berlin, Germany, in 1992 for working on permanent magnet excited machines. After his university studies he worked with the Robert Bosch GmbH in Stuttgart, Germany, as a Design Engineer for Permanent Magnet Servo Motors. From 1988 to 1993 he was a member of staff at the University of Technology Berlin, Germany.

From 1996 to 2004, he was then a Full Professor of Numerical Field Computations and Electrical Machines, Katholieke Universiteit Leuven (KU Leuven), Leuven, Belgium. Since 2004, he has been a Full Professor and the Director of the Institute of Electrical Machines (IEM), RWTH Aachen University, Aachen, Germany.

His research interest focuses on all aspects of the design, control and manufacturing of electrical machines and the associated numerical simulation. The characterization and modeling of hard- and soft-magnetic materials is another focus of his work. He has authored/coauthored more than 350 journal publications, more than 700 international conference publications and four books. His research interests include numerical field computation and optimization, the design and control of electrical machines, in particular, permanent-magnet excited machines, induction machines.

Dr. Hameyer is a member of the German VDE, a Senior Member of IEEE and a Fellow of the Institution of Engineering and Technology, U.K.